ACS EARTH AND SPACE CHEMISTRY

http://pubs.acs.org/journal/aesccq Letter

Mercury Export Flux in the Arctic Ocean Estimated from $^{234}Th/^{238}U$ Disequilibria

Javier A. Tesán Onrubia,[†] Mariia V. Petrova,[†] Viena Puigcorbé, Erin E. Black, Ole Valk, Aurelie Dufour, Bruno Hamelin, Ken O. Buesseler, Pere Masqué, Frederic A. C. Le Moigne, Jeroen E. Sonke, Michiel Rutgers van der Loeff, and Lars-Eric Heimbürger-Boavida*

Cite This: https://dx.doi.org/10.1021/acsearthspacechem.0c00055 Read Online

ACCESS | Metrics & More | Article Recommendations | Supporting Information

ABSTRACT: High mercury (Hg) levels have been observed for arctic biota, despite limited local sources of anthropogenic Hg in the Arctic. Scavenging of Hg exerts an important control on the residence time of Hg in surface waters. The downward Hg export flux and Hg burial rates in bottom sediments are not well-constrained as a result of the lack of particulate Hg (Hg_p) observations in the Arctic Ocean. Here, we estimated downward Hg export flux based on Hg concentrations in suspended particulate matter (SPM) and using the radionuclide pair $^{234}Th/^{238}U$, coupled to $Hg_p/^{234}Th$ ratios in particles. Using new observations made during the German GEOTRACES TransArcII (GN04) and the U.S. Arctic GEOTRACES (GN01) cruises in August−October 2015, we estimated the Hg_p export flux in the central Arctic Ocean and the outer shelf. We find that 81 ± 58 Mg year^{-1} Hg_p is exported from the upper 100 m, of which 16 ± 10 Mg year^{-1} is ultimately buried in marine sediments. An extrapolation to the entire Arctic Ocean, including the inner shelf, results in 156 Mg year^{-1}Hg_p export from the surface ocean and 28 Mg year^{-1} Hg burial rate. Our study shows that the Hg_p export flux could be higher than previously thought, and this should be taken into consideration for future arctic Hg budget estimations.

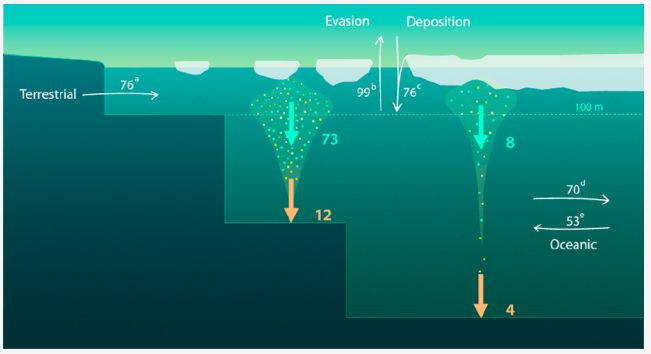

KEYWORDS: *GEOTRACES, particulate mercury, thorium export, particle flux, marine sediment, burial rates, downward flux, contaminant, global change*

Elevated mercury (Hg) levels in arctic biota[1−3] have been explained by enhanced inorganic Hg inputs to the Arctic Ocean.[4,5] Several recent studies aimed at refining Hg inputs from the atmosphere,[6,7] rivers,[8] coastal erosion,[9−11] and other oceans.[12,13] Once delivered to the Arctic Ocean, Hg can undergo complex biotic and abiotic reactions, including the transformation into the bioaccumulative neurotoxin methylmercury (MeHg). Because MeHg is produced at shallow depth in the Arctic Ocean,[14] it is important to know the residence time of Hg, which is largely driven by two removal mechanisms: evasion to the atmosphere and downward export flux with settling particles.

As a result of the high affinity of Hg for particles, scavenging and export flux play a major role in removing Hg from the surface ocean.[15] A fraction of this downward Hg export flux is finally buried in the marine sediments and, in this way, removed from the oceanic Hg budget for millennial time scales. Providing the first comprehensive Arctic Hg budget, Outridge et al.[4] estimated a burial rate of Hg to the marine sediments of 108 Mg year^{-1}. Later on, Soerensen et al.[7] established a box model, which estimates the downward particulate Hg (Hg_p) flux to be 37 Mg year^{-1} and a burial rate of 28 Mg year^{-1} based on the few observations available at the time. Both studies also differ in their estimation of the exchange flux with the atmosphere (Table S1 of the Supporting Information). Outridge et al.[4] find a low Hg evasion flux of 10 Mg year^{-1}, which results in a net atmospheric deposition of 98 Mg year^{-1} to the Arctic Ocean. On the contrary, the box model developed by Soerensen et al.[7] implies that the Arctic Ocean is a Hg source with a net evasion flux to the atmosphere of 23 Mg year^{-1}. The downward Hg export flux from the surface to the deep Arctic Ocean and the Hg burial rate in marine sediments remain poorly constrained (Table S1 of the Supporting Information). Sedimentation rates in the central Arctic Ocean are thought to be very low, and sediment mixing and diagenesis bias the Hg sediment

Special Issue: Marine Particle Chemistry: Influence on Biogeochemical Cycles and Particle Export

Received: February 25, 2020
Revised: April 16, 2020
Accepted: April 22, 2020
Published: April 23, 2020

records.[16] Most sediment traps deployed in the Arctic Ocean use $HgCl_2$ for sample preservation[17] and cannot be used for Hg analysis. Thus far, only one study could provide Hg_p measurements in the central Arctic Ocean.[18]

Previous estimates of Hg fluxes in the Arctic Ocean[4,5,7] had to be based on available information on Hg_p in riverine particles,[19] ice algae,[20] and zooplankton,[21] sediments[16,22] or using partition coefficients (K_d) from the North Atlantic (1.1×10^5 L kg^{-1})[23] or the Pacific Ocean (1×10^6 L kg^{-1}).[24] Fisher et al.[5] used the GEOS-Chem model to explain atmospheric Hg observations in the Arctic. In the absence of Hg_p observations for the Arctic Ocean, this study used K_d from the North Atlantic[23] to estimate the Hg export flux of 43 Mg year^{-1} in the Arctic Ocean. Typically, the GEOS-Chem model uses an average K_d of 3.2×10^5 L kg^{-1} for simulations in other oceans. A recent study, conducted in the North Atlantic by Lamborg et al.,[15] showed that observed K_d values are an order of magnitude higher (4.5×10^6 L kg^{-1}). Soerensen et al.[7] conducted a box model study that suggested that about 37 Mg year^{-1} of Hg is exported below 200 m depth. The authors estimated Hg export fluxes based on particulate fluxes of solids from rivers and erosion (660 Tg year^{-1}) and primary production (1100 Tg year^{-1}, of which 35 Tg year^{-1} is exported below 200 m depth). In the absence of Hg_p data, the authors used a best estimate of 50 ng g^{-1} for all types of particles in the Arctic Ocean.

We used new observations, to develop two different approaches to provide a new estimate for the Hg_p export flux in the central Arctic Ocean and in the outer shelf (>100 m). First, we used new data to calculate Hg_p normalized to suspended particulate matter (Hg_{SPM}) and K_d for the Arctic Ocean. Then, we used Hg_p and ^{234}Th observations, to estimate the Hg_p export flux based on the ^{234}Th/^{238}U disequilibrium.[25] Finally, we re-estimated the net Hg burial rates from our Arctic sediment cores. The data that we used in this study came from two GEOTRACES cruises in 2015 to the Arctic Ocean and that overlapped at the North Pole. The Barents Sea and the central Arctic Ocean were sampled during the GEOTRACES TransArc II (GN04) cruise between August 17th and October 15th, 2015 aboard the FS Polarstern. The western and central Arctic Ocean were sampled during the U.S. Arctic GEOTRACES (GN01) cruise between August 9th and October 12th, 2015. Both ships sampled near the North Pole on September 7th, 2015. For the GN04 cruise, we measured Hg_p concentrations on pre-combusted QMA filters (1−53 μm) mounted on *in situ* pumps deployed at 100 m depth at nine stations. The locations of the stations included permanently ice-covered areas in the central Arctic Ocean (stations 32, 50, 81, 96, 101, and 125) as well as ice-free stations on the shelf of the Barents Sea (stations 4, 153, and 161; Table S2 of the Supporting Information). During the GN01 cruise, Agather et al.[18] measured Hg_p concentrations on QMA filters (1−51 μm) at 100 m depth at nine ice-covered stations in the central Arctic Ocean and one ice-free station on the outer shelf (Table S2 of the Supporting Information).

Particulate Hg concentrations on GN04 averaged 0.097 ± 0.039 pmol L^{-1} (n = 9) and are similar those measured in the western Arctic Ocean during the GN01 cruise (0.072 ± 0.051 pmol L^{-1}; n = 10)[18] but about 3 times higher than Hg_p measured in the North Atlantic.[23,26] The highest Hg_p concentrations were observed over the shelf (GN04, 0.137 ± 0.046 pmol L^{-1}, n = 3; GN01. 0.204 pmol L^{-1}, n = 1), with the lowest off-shore (GN04, 0.076 ± 0.008 pmol L^{-1}, n = 6; GN01, 0.058 ± 0.022 pmol L^{-1}, n = 9). The Hg_p concentrations were converted from water volume (Hg_p in pmol L^{-1}) to particle mass-specific concentrations (Hg_{SPM} in ng g^{-1}), using SPM concentrations from the GN01 cruise for each station at depths between 80 and 120 m.[27] In the absence of SPM measurements on GN04, we applied average values from the GN01 cruise, 9.29 ± 2.28 μg L^{-1} for the central Arctic Ocean and 146 ± 8.46 μg L^{-1} for the outer shelf (Table S2 of the Supporting Information). The Hg_{SPM} concentrations at 100 m depth were 211 ± 69 ng g^{-1} on the shelf and 1484 ± 467 ng g^{-1} in the central Arctic Ocean (Table S2 of the Supporting Information). The Hg_{SPM} concentrations in the central Arctic Ocean were comparable to those measured by Lamborg et al.[15] in the North Atlantic (240−1080 ng g^{-1}) but 4−30 times higher than those by Soerensen et al.[7] for their model. From Hg_{SPM} and dissolved Hg observations, we calculated K_d for each station. The K_d values range from 1.2×10^6 to 1.6×10^7 L kg^{-1}. Our lowest K_d values are 1 order of magnitude higher than the value applied by Fisher et al.[5] in their model (1.1×10^5 L kg^{-1}) and 3 times higher than those determined in the North Atlantic[15] (4.5×10^6 L kg^{-1}; Table S2 of the Supporting Information). Our Hg_{SPM} and K_d values suggest that previous studies may have underestimated Hg export fluxes.

To test this, we used the ^{234}Th /^{238}U deficit measurements to quantify the Hg export flux in the Arctic Ocean. Several studies have employed the ^{234}Th proxy to estimate the particulate flux of trace metals and other compounds.[28−33] Here, we apply for the first time the radionuclide pair ^{234}Th/^{238}U, combined with Hg_p/^{234}Th ratios, to estimate the downward Hg export flux. The half-life of ^{234}Th is 24.1 days and is highly particle-reactive, with K_d values (~10^6−10^7)[34] similar to those of Hg in oxygenated seawater.[15] The relatively short half-life of ^{234}Th makes it a suitable tracer to examine biologically mediated temporal changes in particulate organic carbon (POC) production and export, using the POC/^{234}Th ratio in the particles to convert the ^{234}Th export flux to POC export flux.[25,35] Similarly, here, we measured the Hg_p/^{234}Th ratios on filtered particulates (1−51 or 53 μm) to convert the ^{234}Th flux to the Hg_p flux, assuming that the Hg_p/^{234}Th ratios in those particles are equivalent to the ratios on the sinking particles driving Hg_p export. We chose to sample at 100 m depth within the halocline, well below the polar mixed layer (typically 20 m) and above the Atlantic-sourced waters (typically 150−700 m depth). The particulate ^{234}Th activities measured during the GN04 and GN01 cruises averaged 0.24 ± 0.16 dpm L^{-1} (range of 0.067−0.76 dpm L^{-1}; n = 19; Table S2 of the Supporting Information). We calculated ^{234}Th export flux at 100 m depth, which ranged between −300 ± 100 and 569 ± 207 dpm m^{-2} day^{-1} in the central Arctic Ocean and between 221 ± 175 and 700 ± 100 dpm m^{-2} day^{-1} on the shelf (Table S2 of the Supporting Information). Negative values are considered to be negligible and equal to zero, which might be caused by remineralization, lateral advection,[36,37] and/or inputs of ^{234}Th-enriched ice algae.[38] Low (or negligible) ^{234}Th export fluxes are common in the Arctic Ocean,[39] particularly at the end of summer when the cruises took place, as a result of low productivity and a community structure that does not promote efficient export. The average Hg_p/^{234}Th ratio was 0.48 ± 0.31 pmol dpm^{-1} (range of 0.072−1.05 pmol dpm^{-1}; n = 19; Table S2 of the Supporting Information). On the basis of the measured Hg_p/^{234}Th ratios, we estimated the Hg export fluxes at each station, which were

https://dx.doi.org/10.1021/acsearthspacechem.0c00055
ACS Earth Space Chem. XXXX, XXX, XXX−XXX

lower in the permanently ice-covered central Arctic Ocean and higher over the outer shelf (Table S2 of the Supporting Information). Applying the average $Hg_p/^{234}Th$ ratio measured during GN01 and GN04 to the ^{234}Th fluxes reported in the current and previous studies,[39−47] we estimated the Hg export fluxes below 100 m depth for different locations in the central Arctic Ocean and outer shelf zones (Figure 1). The lowest Hg_p

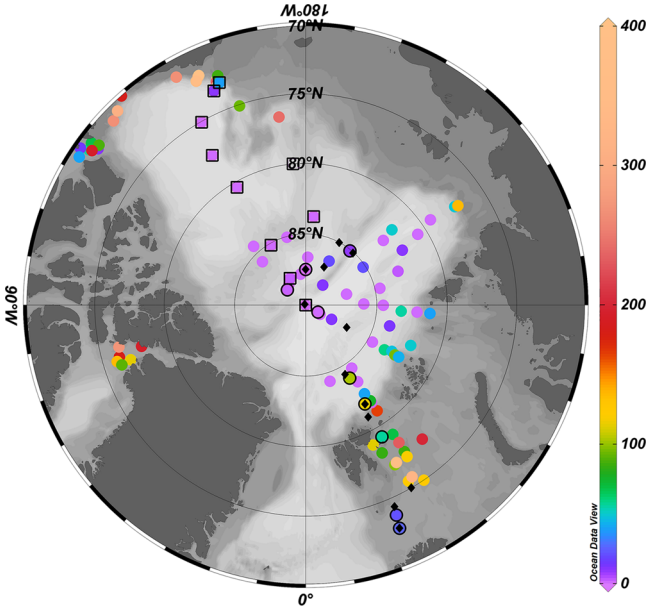

Figure 1. Particulate Hg export fluxes at 100 m depth (pmol $m^{-2}day^{-1}$) derived from the ^{234}Th approach and the $Hg_p/^{234}Th$ ratios from this study. Negative fluxes were considered equal to zero. Black circles and squares indicate stations from the GN04 and GN01 cruises, respectively. Black diamonds indicate stations from GN04 where sediment cores were collected. The other data points have been calculated using previously published ^{234}Th fluxes[39−47] and the average $Hg_p/^{234}Th$ ratio obtained in this study.

export fluxes were found in the permanently ice-covered central Arctic Ocean (average of 95 ± 195 pmol m^{-2} day^{-1}; n = 49), while the highest Hg_p export fluxes were found in the outer shelf (average of 635 ± 480 pmol m^{-2} day^{-1}; n = 50; Figure 1). Our Hg_p export flux estimates for the central Arctic Ocean are comparable to observations in the Pacific Ocean based on sediment trap deployments (157 ± 48 pmol m^{-2} day^{-1}).[48] However, we observe higher Hg_p export flux on the productive outer shelf. Our assessment might be slightly biased by seasonal and long-term variability, because some of the used literature ^{234}Th export fluxes were obtained during different seasons and years. Similar to our study, some of the previously reported values indicated negligible ^{234}Th export fluxes.[39−47]

To estimate the annual export flux of Hg, we used a primary production period of 85 days for the central Arctic Ocean and 190 days for the outer shelf[49,50] and surface areas for the central Arctic Ocean and the outer shelf of 5×10^6 and 3×10^6 km^2, respectively. On the basis of this assumption, we estimated that 8 ± 17 Mg $year^{-1}$ of Hg are exported below 100 m depth in the central Arctic Ocean and 73 ± 55 Mg $year^{-1}$ over the outer shelf (Figure 2). The fact that most of the Hg export takes place over the outer shelf is likely related to the enhanced primary productivity compared to the central arctic basin waters.[51] Several studies already reported high uncertainties of ^{234}Th-derived C and trace metal fluxes.[33,52,53]

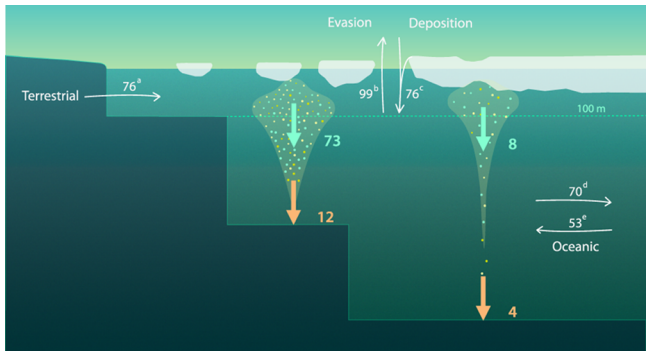

Figure 2. Mass balance of Hg in the Arctic Ocean with flux (Mg $year^{-1}$) components estimated in this study: export fluxes at 100 m depth (labeled as green arrows) and net burial fluxes (labeled as orange arrows) combined with fluxes described by Soerensen et al.[7] (a, b, c, and d), Sonke et al.[8] (a), Petrova et al.[13] (d and e).

We estimated a lower boundary for the Hg_p export flux from surface water with 81 ± 58 Mg $year^{-1}$. If we assume that fluxes on the inner shelf (<100 m depth), which represents about 25% of the Arctic Ocean surface and receives direct Hg and nutrients inputs via river runoff and coastal erosion,[7,8] were similar to those of the outer shelf, extrapolated from the inner shelf, annual flux for the entire Arctic Ocean is about 156 Mg $year^{-1}$.

Settling particles are remineralized during their downward flux, and only a small portion is finally buried in marine sediments.[54] To check how this affects Hg export flux, we measured Hg_p concentrations in sediments collected during the GN04 cruise on the outer shelf and central Arctic Ocean (Figure 1). We used our data and previous Hg_p observations (upper 0.5−2 cm; Table S3 of the Supporting Information)[16,55−58] to estimate the net Hg burial rates. On the basis of sedimentation rates typically found in the Arctic Ocean (0.03 mm $year^{-1}$) and for the open ocean and outer shelf (0.3 mm $year^{-1}$) following Soerensen et al.,[7] we calculated average Hg burial rates of 11 ± 8 and 51 ± 35 pmol m^{-2} day^{-1}, respectively. Considering the surface area of the central Arctic Ocean and outer shelf with 5×10^6 and 3×10^6 km^2, respectively, we estimated Hg burial rates of 4 ± 3 Mg $year^{-1}$ in the central Arctic Ocean and 12 ± 7 Mg $year^{-1}$ in the deep shelf (Table S3 of the Supporting Information). Our new estimates are slightly lower than those by Soerensen et al.[7] (3 and 25 Mg $year^{-1}$, respectively). In the absence of Hg_p observations on the inner shelf, our Hg burial rate of 16 ± 10 Mg $year^{-1}$ for the Arctic Ocean is a lower boundary, and an extrapolation for the entire Arctic Ocean results in the same overall value (28 Mg $year^{-1}$) as found by Soerensen et al.[7]. If we were to compare our results (51 ± 35 pmol m^{-2} day^{-1}) to another semi-enclosed basin, the Mediterranean Sea, with sedimentation rates (0.4 mm $year^{-1}$) similar to the arctic outer shelf (0.3 mm $year^{-1}$), we find lower Hg burial rates than 115 pmol m^{-2} day^{-1}.[54] The high range of observed sedimentation rates, 0.0025−0.05 mm $year^{-1}$ for the central Arctic Ocean and 0.1−2.5 mm $year^{-1}$ for the shelf,[59−61] also results in a high uncertainty in the Hg burial rate estimates.

We used our new estimates of Hg_p downward export and the Hg burial fluxes combined with current observations and modeling studies[7,8,13] to refine our understanding of the Hg cycle in the Arctic Ocean (Figure 2). On the basis of our Hg observations on SPM and sediments, we calculate that 5.6 ± 2.9% of exported Hg_p from the upper 100 m depth is

https://dx.doi.org/10.1021/acsearthspacechem.0c00055
ACS Earth Space Chem. XXXX, XXX, XXX−XXX

ultimately buried in the central Arctic sediments. Most of the Hg_p downward flux is remineralized below 100 m depth, which is also suggested by the $^{234}Th/^{238}U$ profiles (Viena Puigcorbé, personal communication; data not shown here). We hypothesize that Hg_p exported below 100 m depth may contribute to the shallow production of MeHg in the Arctic Ocean.[2,14,18,62] Post-depositional diagenetic processes lead to epibenthic mobilization of dissolved Hg species to overlaying seawater. Heimbürger et al.[54] found that epibenthic mobilization of Hg can explain 73% of the observed difference between water column export flux and Hg burial. Our study could not address the possible influence of nycthemeral zooplankton dynamics, convective SPM, and diffusive fluxes. Cascading processes, which take place on the shelf by the downwelling of waters,[63] may also be an important pathway for Hg_p and ^{234}Th displacement from shallow to deep waters.

About 76 Mg $year^{-1}$ of Hg has been suggested to be transported to the Arctic shelves by rivers or sourced from coastal erosion.[7,8] The high sensitivity of the Arctic to climate change can perturb Arctic Hg cycling, increasing land to ocean Hg export fluxes because permafrost thawing and extreme weather events are expected to deliver important amounts of Hg to Arctic Ocean.[64] In addition, the increase of the open water season as a result of ice retreat is leading to an increase of net primary production,[65] also enhancing Hg scavenging and downward export, which would reduce the amount of Hg available for MeHg production. However, a shift to small-sized phytoplankton may lead to increased MeHg production.[14] Only continued seasonal and long-term arctic surveys will allow for the building of a first time series and the making of coherent future projections.

About half of the Arctic shelf is shallower than 100 m (inner shelf) and could not be addressed by our study. We can only provide approximate Hg_p export fluxes below 100 m depth for the outer shelf and the central Arctic Ocean. The use of the $Hg_p/^{234}Th$ ratio in particles to obtain Hg export flux should be further developed and expanded to other oceans. In particular, future research should address the spatial and temporal variability of the $Hg_p/^{234}Th$ ratio considering biogeochemical regions and seasonality. Ongoing climate change impacts to the Arctic Ocean ecosystem should also be assessed, including changes in sea ice cover, particle and nutrient supply, primary productivity, and hydrological circulations, which will likely impact Hg_p export and overall Hg budget in the Arctic Ocean.

METHODS

We used Hg_p from the GN01 cruise, for which information on the measurement details are given by Agather et al.[18] We obtained the data set upon request from Alison Agather by personal e-mail and should become available on https://www.bco-dmo.org/dataset/738307. Particles were collected using McLane *in situ* pumps (LV08) equipped with a pre-filter (screen) of 51 or 53 μm pore size (for GN01 and GN04, respectively), followed by a pre-combusted QMA filter from where the samples for this study were collected (i.e., particle size sampled 1−51 or 53 μm). For both cruises, particulate ^{234}Th and Hg_p were measured from the exact same filter. Punches (25 mm) were subsampled from each filter for particulate ^{234}Th, dried overnight at 50 °C, counted on board, and recounted again 6 months later for background corrections. After the second counting, the POC content was analyzed in the same filters with an EuroVector elemental analyzer (Euroanalysator EA).

During the GN04 cruise Hg_p, the remainder of the filters were kept frozen at −20 °C until analyses for Hg_p. A total of 12 sediment cores were recovered using the trace metal clean NIOZ minicorer. Sediment cores were sliced every 5 mm using a Plexiglas spatula. Only the upper 5 mm was considered for the estimation of Hg burial rates. The sediment samples were kept frozen at −20 °C until analyses for Hg_p. All samples were freeze-dried (Christ Gamma 1-16 LSCplus), and 25 mm diameter punch-out samples were analyzed using a CV-AAS (LECO AMA 254) equipped with a low Hg optical cell. The limit of detection, estimated as 3 times the standard deviation of the blank samples, was 1.2 pg, which was equivalent to about 0.0001 pM, considering the filtered amount of seawater (289−599 L).

Total ^{234}Th activities were determined from 4 L of seawater collected at 18−20 depths (GN04) or 10−15 depths (GN01) in the upper ∼400 m of the water column. Replicates of deep samples (GN04, 3000 m; GN01, 2000 m) were collected for calibration purposes.[66] The samples were processed following the MnO_2 co-precipitation technique[67] using ^{230}Th as a chemical yield tracer.[68] The counting was performed on board using low-background β counters and measured again 6 months later for background quantification, as per particulate ^{234}Th samples. Recoveries for ^{234}Th were determined on all filters by inductively coupled plasma mass spectrometry with an average recovery of 0.87 ± 0.03 (GN04; n = 225).

ASSOCIATED CONTENT

Supporting Information

The Supporting Information is available free of charge at https://pubs.acs.org/doi/10.1021/acsearthspacechem.0c00055.

> Comparison of some Hg fluxes in the Arctic Ocean available from Outridge et al., Fisher et al., and Soerensen et al. (Table S1), Hg_p and ^{234}Th activities measured on small fraction (1−51 or 53 μm), ^{234}Th export fluxes at 100 m depth, $Hg_p/^{234}Th$ ratios (pmol dpm^{-1}) measured on small particles (1−51 or 53 μm), and ^{234}Th-derived Hg fluxes at 100 m depth measured during the GN04 and GN01 cruises (Table S2), and average Hg_p concentrations (ng g^{-1}), dry sediment density (g cm^{-3}), and estimated Hg burial rates (pmol m^{-2} day^{-1} and Mg $year^{-1}$) for the outer shelf and central Arctic Ocean (Table S3) (PDF)

AUTHOR INFORMATION

Corresponding Author

Lars-Eric Heimbürger-Boavida − *Aix Marseille Université, CNRS/INSU, Université de Toulon, IRD, Mediterranean Institute of Oceanography, 13288 Marseilles, France;* orcid.org/0000-0003-0632-5183; Email: lars-eric.heimburger@mio.osupytheas.fr

Authors

Javier A. Tesán Onrubia − *Aix Marseille Université, CNRS/INSU, Université de Toulon, IRD, Mediterranean Institute of Oceanography, 13288 Marseilles, France*

Mariia V. Petrova − *Aix Marseille Université, CNRS/INSU, Université de Toulon, IRD, Mediterranean Institute of Oceanography, 13288 Marseilles, France*

https://dx.doi.org/10.1021/acsearthspacechem.0c00055
ACS Earth Space Chem. XXXX, XXX, XXX−XXX

Viena Puigcorbé − *School of Science, Centre for Marine Ecosystems Research, Edith Cowan University, Joondalup, Western Australia 6027, Australia*
Erin E. Black − *Ocean Frontier Institute, Dalhousie University, Halifax, Nova Scotia B3H 4R2, Canada; Lamont-Doherty Earth Observatory, Palisades, New York 10964, United States*
Ole Valk − *Alfred Wegener Institute Helmholtz Centre for Polar and Marine Research, 27570 Bremerhaven, Germany*
Aurelie Dufour − *Aix Marseille Université, CNRS/INSU, Université de Toulon, IRD, Mediterranean Institute of Oceanography, 13288 Marseilles, France*
Bruno Hamelin − *Aix Marseille Université, CNRS, IRD, INRA, Coll France, CEREGE, 13545 Aix en Provence, France*
Ken O. Buesseler − *Woods Hole Oceanographic Institution, Woods Hole, Massachusetts 02543, United States*
Pere Masqué − *School of Science, Centre for Marine Ecosystems Research, Edith Cowan University, Joondalup, Western Australia 6027, Australia; Institut de Ciència i Tecnologia Ambientals and Departament de Física, Universitat Autònoma de Barcelona, 08193 Barcelona, Spain; International Atomic Energy Agency, 98000 Principality of Monaco, Monaco*
Frederic A. C. Le Moigne − *Aix Marseille Université, CNRS/INSU, Université de Toulon, IRD, Mediterranean Institute of Oceanography, 13288 Marseilles, France*
Jeroen E. Sonke − *Laboratoire Géosciences Environnement Toulouse, CNRS/IRD/CNES/Université Paul Sabatier−Toulouse III, 31400 Toulouse, France;* orcid.org/0000-0001-7146-3035
Michiel Rutgers van der Loeff − *Alfred Wegener Institute Helmholtz Centre for Polar and Marine Research, 27570 Bremerhaven, Germany*

Complete contact information is available at: https://pubs.acs.org/10.1021/acsearthspacechem.0c00055

Author Contributions

[†]Javier A. Tesán Onrubia and Mariia V. Petrova contributed equally to this work.

Notes

The authors declare no competing financial interest.

■ ACKNOWLEDGMENTS

The authors thank the editor, Joel D. Blum, and the anonymous reviewers for the constructive suggestions and comments. The authors thank Alison Agather and Phoebe J. Lam for making the GN01 Hg_p and SPM data available. The authors also thank the chief scientists Ursula Schauer, Dave Kadko, and William Landing, captains, officers, and crew of the FS Polarstern and the USCGC Healy. The authors thank the CNRS Chantier Arctique Français funding via the Pollution in the Arctic System Project, the European Research Council (ERC-2010-StG_20091028) to Jeroen E. Sonke, and the AXA Research Fund to Lars-Eric Heimbürger-Boavida (Postdoc Grant Levering Knowledge Gaps To Understand and Anticipate Risk from Methylmercury Exposure and Outreach Grant Arctic Mediterranean Mercury). The authors also thank a National Aeronautics and Space Administration (NASA) Earth and Space Science Fellowship Program Grant (NNX13AP31H) and the National Science Foundation (OCE-1458305) funding to Erin E. Black and Ken O. Buesseler. The authors are thankful to Sandra Gdaniec for her support with the *in situ* pump sampling and Walter Geibert for the thorium recovery analyses. The International Atomic Energy Agency (IAEA) is grateful for the support provided to its Environment Laboratories by the Government of the Principality of Monaco. Pere Masqué acknowledges the support of the Generalitat de Catalunya (MERS 2017 SGR-1588). This work contributes to the ICTA Unit of Excellence (MinECo, MDM2015-0552). The authors also thank Itziar Tesán for the support with a graphical design.

■ REFERENCES

(1) Dietz, R.; Sonne, C.; Basu, N.; Braune, B.; O'Hara, T.; Letcher, R. J.; Scheuhammer, T.; Andersen, M.; Andreasen, C.; Andriashek, D.; Asmund, G.; Aubail, A.; Baagøe, H.; Born, E. W.; Chan, H. M.; Derocher, A. E.; Grandjean, P.; Knott, K.; Kirkegaard, M.; Krey, A.; Lunn, N.; Messier, F.; Obbard, M.; Olsen, M. T.; Ostertag, S.; Peacock, E.; Renzoni, A.; Rigét, F. F.; Skaare, J. U.; Stern, G.; Stirling, I.; Taylor, M.; Wiig, Ø.; Wilson, S.; Aars, J. What Are the Toxicological Effects of Mercury in Arctic Biota? *Sci. Total Environ.* **2013**, *443*, 775−790.
(2) Wang, K.; Munson, K. M.; Beaupré-Laperrière, A.; Mucci, A.; Macdonald, R. W.; Wang, F. Subsurface Seawater Methylmercury Maximum Explains Biotic Mercury Concentrations in the Canadian Arctic. *Sci. Rep.* **2018**, *8* (1), 14465.
(3) Dudarev, A.; Chupakhin, V.; Vlasov, S.; Yamin-Pasternak, S. Traditional Diet and Environmental Contaminants in Coastal Chukotka III: Metals. *Int. J. Environ. Res. Public Health* **2019**, *16* (5), 699.
(4) Outridge, P. M.; Macdonald, R. W.; Wang, F.; Stern, G. A.; Dastoor, A. P. A Mass Balance Inventory of Mercury in the Arctic Ocean. *Environmental Chemistry* **2008**, *5* (2), 89.
(5) Fisher, J. A.; Jacob, D. J.; Soerensen, A. L.; Amos, H. M.; Steffen, A.; Sunderland, E. M. Riverine Source of Arctic Ocean Mercury Inferred from Atmospheric Observations. *Nat. Geosci.* **2012**, *5* (7), 499−504.
(6) Schroeder, W. H.; Anlauf, K. G.; Barrie, L. A.; Lu, J. Y.; Steffen, A.; Schneeberger, D. R.; Berg, T. Arctic Springtime Depletion of Mercury. *Nature* **1998**, *394* (6691), 331−332.
(7) Soerensen, A. L.; Jacob, D. J.; Schartup, A. T.; Fisher, J. A.; Lehnherr, I.; St. Louis, V. L.; Heimbürger, L. E.; Sonke, J. E.; Krabbenhoft, D. P.; Sunderland, E. M. A Mass Budget for Mercury and Methylmercury in the Arctic Ocean: Arctic Ocean Hg and MeHg mass budget. *Global Biogeochem. Cycles* **2016**, *30* (4), 560−575.
(8) Sonke, J. E.; Teisserenc, R.; Heimbürger-Boavida, L. E.; Petrova, M. V.; Marusczak, N.; Le Dantec, T.; Chupakov, A. V.; Li, C.; Thackray, C. P.; Sunderland, E. M.; Tananaev, N.; Pokrovsky, O. S. Eurasian River Spring Flood Observations Support Net Arctic Ocean Mercury Export to the Atmosphere and Atlantic Ocean. *Proc. Natl. Acad. Sci. U. S. A.* **2018**, *115* (50), E11586−E11594.
(9) Leitch, D. R.; Carrie, J.; Lean, D.; Macdonald, R. W.; Stern, G. A.; Wang, F. The Delivery of Mercury to the Beaufort Sea of the Arctic Ocean by the Mackenzie River. *Sci. Total Environ.* **2007**, *373* (1), 178−195.
(10) Schuster, P. F.; Schaefer, K. M.; Aiken, G. R.; Antweiler, R. C.; Dewild, J. F.; Gryziec, J. D.; Gusmeroli, A.; Hugelius, G.; Jafarov, E.; Krabbenhoft, D. P.; Liu, L.; Herman-Mercer, N.; Mu, C.; Roth, D. A.; Schaefer, T.; Striegl, R. G.; Wickland, K. P.; Zhang, T. Permafrost Stores a Globally Significant Amount of Mercury. *Geophys. Res. Lett.* **2018**, *45* (3), 1463−1471.
(11) Lim, A. G.; Jiskra, M.; Sonke, J. E.; Loiko, S. V.; Kosykh, N.; Pokrovsky, O. S. A Revised Northern Soil Hg Pool, Based on Western Siberia Permafrost Peat Hg and Carbon Observations. *Biogeosciences* **2020**, DOI: 10.5194/bg-2019-483.
(12) Cossa, D.; Heimbürger, L. E.; Pérez, F. F.; García-Ibáñez, M. I.; Sonke, J. E.; Planquette, H.; Lherminier, P.; Boutorh, J.; Cheize, M.; Menzel Barraqueta, J. L.; Shelley, R.; Sarthou, G. Mercury Distribution and Transport in the North Atlantic Ocean along the GEOTRACES-GA01 Transect. *Biogeosciences* **2018**, *15* (8), 2309−2323.

(13) Petrova, M. V.; Krisch, S.; Lodeiro, P.; Valk, O.; Dufour, A.; Rijkenberg, M. J. A.; Takamasa; Achtenberg, E. P.; Rabe, B.; van der Loeff, M. R.; Hamelin, B.; Sonke, J. E.; Garnier, C.; Heimbürger-Boavida, L. E. Arctic Ocean exports methylmercury to the Atlantic Ocean. *Marine Chemistry*, submitted.
(14) Heimbürger, L. E.; Sonke, J. E.; Cossa, D.; Point, D.; Lagane, C.; Laffont, L.; Galfond, B. T.; Nicolaus, M.; Rabe, B.; van der Loeff, M. R. Shallow Methylmercury Production in the Marginal Sea Ice Zone of the Central Arctic Ocean. *Sci. Rep.* **2015**, *5*, 10318.
(15) Lamborg, C. H.; Hammerschmidt, C. R.; Bowman, K. L. An Examination of the Role of Particles in Oceanic Mercury Cycling. *Philos. Trans. R. Soc., A* **2016**, *374* (2081), 20150297.
(16) Gobeil, C.; Macdonald, R. W.; Smith, J. N. Mercury Profiles in Sediments of the Arctic Ocean Basins. *Environ. Sci. Technol.* **1999**, *33* (23), 4194−4198.
(17) Kraft, A.; Bauerfeind, E.; Nöthig, E.-M.; Klages, M.; Beszczynska-Möller, A.; Bathmann, U. V. Amphipods in Sediment Traps of the Eastern Fram Strait with Focus on the Life-History of the Lysianassoid Cyclocaris Guilelmi. *Deep Sea Res., Part I* **2013**, *73*, 62−72.
(18) Agather, A. M.; Bowman, K. L.; Lamborg, C. H.; Hammerschmidt, C. R. Distribution of Mercury Species in the Western Arctic Ocean (U.S. GEOTRACES GN01). *Mar. Chem.* **2019**, *216*, 103686.
(19) Graydon, J. A.; Emmerton, C. A.; Lesack, L. F. W.; Kelly, E. N. Mercury in the Mackenzie River Delta and Estuary: Concentrations and Fluxes during Open-Water Conditions. *Sci. Total Environ.* **2009**, *407* (8), 2980−2988.
(20) Burt, A. E. Mercury uptake and dynamics in sea ice algae, phytoplankton and grazing copepods from a Beaufort Sea Arctic marine food web. M.S. Thesis, University of Manitoba, Winnipeg, Manitoba, Canada, 2012; http://hdl.handle.net/1993/8907.
(21) Pućko, M.; Burt, A.; Walkusz, W.; Wang, F.; Macdonald, R. W.; Rysgaard, S.; Barber, D. G.; Tremblay, J.-É.; Stern, G. A. Transformation of Mercury at the Bottom of the Arctic Food Web: An Overlooked Puzzle in the Mercury Exposure Narrative. *Environ. Sci. Technol.* **2014**, *48* (13), 7280−7288.
(22) Macdonald, R. W.; Thomas, D. J. Chemical Interactions and Sediments of the Western Canadian Arctic Shelf. *Cont. Shelf Res.* **1991**, *11* (8−10), 843−863.
(23) Mason, R. P.; Rolfhus, K. R.; Fitzgerald, W. F. Mercury in the North Atlantic. *Mar. Chem.* **1998**, *61* (1−2), 37−53.
(24) Mason, R. P.; Fitzgerald, W. F. The Distribution and Biogeochemical Cycling of Mercury in the Equatorial Pacific Ocean. *Deep Sea Res., Part I* **1993**, *40* (9), 1897−1924.
(25) Coale, K. H.; Bruland, K. W. ^{234}Th:^{238}U Disequilibria within the California Current. *Limnol. Oceanogr.* **1985**, *30* (1), 22−33.
(26) Bowman, K. L.; Hammerschmidt, C. R.; Lamborg, C. H.; Swarr, G. Mercury in the North Atlantic Ocean: The U.S. GEOTRACES Zonal and Meridional Sections. *Deep Sea Res., Part II* **2015**, *116*, 251−261.
(27) Lam, P. J. *Size-Fractionated Major and Minor Particle Composition and Concentration from the US GEOTRACES Arctic Cruise (HLY1502) on USCGC Healy from August to October 2015*; Biological and Chemical Oceanography Data Management Office (BCO-DMO): Woods Hole, MA, 2020; Dataset Version 2020-04-01, DOI: 10.26008/1912/bco-dmo.807340.1.
(28) Dulaquais, G.; Boye, M.; Middag, R.; Owens, S.; Puigcorbe, V.; Buesseler, K.; Masqué, P.; de Baar, H. J. W.; Carton, X. Contrasting Biogeochemical Cycles of Cobalt in the Surface Western Atlantic Ocean: Surface Biogeochemical Cycles Of Cobalt. *Global Biogeochemical Cycles* **2014**, *28* (12), 1387−1412.
(29) Gustafsson, Ö.; Gschwend, P. M.; Buesseler, K. O. Settling Removal Rates of PCBs into the Northwestern Atlantic Derived from ^{238}U−^{234}Th Disequilibria. *Environ. Sci. Technol.* **1997**, *31* (12), 3544−3550.
(30) Gustafsson, Ö.; Gschwend, P. M.; Buesseler, K. O. Using ^{234}Th Disequilibria to Estimate the Vertical Removal Rates of Polycyclic Aromatic Hydrocarbons from the Surface Ocean. *Mar. Chem.* **1997**, *57* (1−2), 11−23.
(31) Weinstein, S. E.; Moran, S. B. Vertical Flux of Particulate Al, Fe, Pb, and Ba from the Upper Ocean Estimated from ^{234}Th/^{238}U Disequilibria. *Deep Sea Res., Part I* **2005**, *52* (8), 1477−1488.
(32) Hayes, C. T.; Black, E. E.; Anderson, R. F.; Baskaran, M.; Buesseler, K. O.; Charette, M. A.; Cheng, H.; Cochran, J. K.; Edwards, R. L.; Fitzgerald, P.; Lam, P. J.; Lu, Y.; Morris, S. O.; Ohnemus, D. C.; Pavia, F. J.; Stewart, G.; Tang, Y. Flux of Particulate Elements in the North Atlantic Ocean Constrained by Multiple Radionuclides. *Global Biogeochem. Cycles* **2018**, *32* (12), 1738−1758.
(33) Black, E. E.; Lam, P. J.; Lee, J.-M.; Buesseler, K. O. Insights from the ^{238}U−^{234}Th Method into the Coupling of Biological Export and the Cycling of Cadmium, Cobalt, and Manganese in the Southeast Pacific Ocean. *Global Biogeochem. Cycles* **2019**, *33* (1), 15−36.
(34) International Atomic Energy Agency (IAEA). *Sediment Kd's and Concentration Factors for Radionuclides in the Marine Environment*; IAEA: Vienna, Austria, 1985; Technical Reports Series 247.
(35) Buesseler, K. O.; Bacon, M. P.; Kirk Cochran, J.; Livingston, H. D. Carbon and Nitrogen Export during the JGOFS North Atlantic Bloom Experiment Estimated from ^{234}Th:^{238}U Disequilibria. Deep Sea Research Part A. *Deep-Sea Res., Part A* **1992**, *39* (7−8), 1115−1137.
(36) Savoye, N.; Buesseler, K. O.; Cardinal, D.; Dehairs, F. ^{234}Th Deficit and Excess in the Southern Ocean during Spring 2001: Particle Export and Remineralization: S.O. Particle Export and Remineralization. *Geophys. Res. Lett.* **2004**, *31* (12), L12301.
(37) Maiti, K.; Benitez-Nelson, C. R.; Buesseler, K. O. Insights into Particle Formation and Remineralization Using the Short-Lived Radionuclide, Thorium-234: Particle Remineralization Using Th-234. *Geophys. Res. Lett.* **2010**, *37* (15), L15608.
(38) Rodriguez y Baena, A. M.; Boudjenoun, R.; Fowler, S. W.; Miquel, J. C.; Masqué, P.; Sanchez-Cabeza, J.-A.; Warnau, M. ^{234}Th-Based Carbon Export during an Ice-Edge Bloom: Sea-Ice Algae as a Likely Bias in Data Interpretation. *Earth Planet. Sci. Lett.* **2008**, *269* (3−4), 596−604.
(39) Roca-Martí, M.; Puigcorbé, V.; Rutgers van der Loeff, M. M.; Katlein, C.; Fernández-Méndez, M.; Peeken, I.; Masqué, P. Carbon Export Fluxes and Export Efficiency in the Central Arctic during the Record Sea-Ice Minimum in 2012: A Joint ^{234}Th/^{238}U and ^{210}Po/^{210}Pb Study: POC Fluxes In The Central Arctic In 2012. *J. Geophys. Res.: Oceans* **2016**, *121* (7), 5030−5049.
(40) Amiel, D.; Cochran, J. K.; Hirschberg, D. J. ^{234}Th/^{238}U Disequilibrium as an Indicator of the Seasonal Export Flux of Particulate Organic Carbon in the North Water. *Deep Sea Res., Part II* **2002**, *49* (22−23), 5191−5209.
(41) Coppola, L.; Roy-Barman, M.; Wassmann, P.; Mulsow, S.; Jeandel, C. Calibration of Sediment Traps and Particulate Organic Carbon Export Using ^{234}Th in the Barents Sea. *Mar. Chem.* **2002**, *80* (1), 11−26.
(42) Chen, M.; Huang, Y.; Cai, P.; Guo, L. Particulate Organic Carbon Export Fluxes in The Canada Basin and Bering Sea as Derived from ^{234}Th/^{238}U Disequilibria. *Arctic* **2003**, *56* (1), 1−109.
(43) Qiang, M.; Min, C.; Yusheng, Q.; Yanping, L. I. Regional estimates of POC export flux derived from thorium-234 in the western Arctic Ocean. *Acta Oceanol. Sin.* **2005**, *24* (6), 97−108.
(44) Lalande, C.; Lepore, K.; Cooper, L. W.; Grebmeier, J. M.; Moran, S. B. Export Fluxes of Particulate Organic Carbon in the Chukchi Sea: A Comparative Study Using ^{234}Th/^{238}U Disequilibria and Drifting Sediment Traps. *Mar. Chem.* **2007**, *103* (1−2), 185−196.
(45) Amiel, D.; Cochran, J. K. Terrestrial and Marine POC Fluxes Derived from ^{234}Th Distributions and δ^{13}C Measurements on the Mackenzie Shelf. *J. Geophys. Res.: Oceans* **2008**, *113* (C3), C03S06.
(46) Lalande, C.; Moran, S. B.; Wassmann, P.; Grebmeier, J. M.; Cooper, L. W. ^{234}Th-Derived Particulate Organic Carbon Fluxes in the Northern Barents Sea with Comparison to Drifting Sediment Trap Fluxes. *J. Mar. Syst.* **2008**, *73* (1−2), 103−113.

(47) Cai, P.; Rutgers van der Loeff, M.; Stimac, I.; Nöthig, E.-M.; Lepore, K.; Moran, S. B. Low Export Flux of Particulate Organic Carbon in the Central Arctic Ocean as Revealed by ^{234}Th:^{238}U Disequilibrium. *J. Geophys. Res.: Oceans* **2010**, *115* (C10), C10037.
(48) Munson, K. M.; Lamborg, C. H.; Swarr, G. J.; Saito, M. A. Mercury Species Concentrations and Fluxes in the Central Tropical Pacific Ocean: Central Pacific Mercury. *Global Biogeochemical Cycles* **2015**, *29* (5), 656−676.
(49) Strass, V. H.; Nöthig, E.-M. Seasonal Shifts in Ice Edge Phytoplankton Blooms in the Barents Sea Related to the Water Column Stability. *Polar Biol.* **1996**, *16* (6), 409−422.
(50) Niebauer, H. J. An Update on the Climatology and Sea Ice of the Bering Sea. In *Dynamics of the Bering Sea: A Summary of Physical, Chemical and Biological Characteristics and a Synopsis of Research*; Loughlin, T. R., Ohtani, K., Eds.; University of Alaska Sea Grant: Fairbanks, AK, 1999.
(51) Sakshaug, E. Primary and Secondary Production in the Arctic Seas. In *The Organic Carbon Cycle in the Arctic Ocean*; Stein, R., MacDonald, R. W., Eds.; Springer: Berlin, Germany, 2004; Chapter 3, pp 57−81, DOI: 10.1007/978-3-642-18912-8_3.
(52) Puigcorbé, V.; Roca-Martí, M.; Masqué, P.; Benitez-Nelson, C.; Rutgers van der Loeff, M.; Bracher, A.; Moreau, S. Latitudinal Distributions of Particulate Carbon Export across the North Western Atlantic Ocean. *Deep Sea Res., Part I* **2017**, *129*, 116−130.
(53) Le Moigne, F. A. C.; Henson, S. A.; Sanders, R. J.; Madsen, E. Global Database of Surface Ocean Particulate Organic Carbon Export Fluxes Diagnosed from the ^{234} Th Technique. *Earth System Science Data* **2013**, *5* (2), 295−304.
(54) Heimbürger, L. E.; Cossa, D.; Thibodeau, B.; Khripounoff, A.; Mas, V.; Chiffoleau, J.-F.; Schmidt, S.; Migon, C. Natural and Anthropogenic Trace Metals in Sediments of the Ligurian Sea (Northwestern Mediterranean). *Chem. Geol.* **2012**, *291*, 141−151.
(55) Trefry, J. H.; Rember, R. D.; Trocine, R. P.; Brown, J. S. Trace Metals in Sediments near Offshore Oil Exploration and Production Sites in the Alaskan Arctic. *Environ. Geol.* **2003**, *45* (2), 149−160.
(56) Hare, A. A.; Stern, G. A.; Kuzyk, Z. Z. A.; Macdonald, R. W.; Johannessen, S. C.; Wang, F. Natural and Anthropogenic Mercury Distribution in Marine Sediments from Hudson Bay, Canada. *Environ. Sci. Technol.* **2010**, *44* (15), 5805−5811.
(57) Fox, A. L.; Hughes, E. A.; Trocine, R. P.; Trefry, J. H.; Schonberg, S. V.; McTigue, N. D.; Lasorsa, B. K.; Konar, B.; Cooper, L. W. Mercury in the Northeastern Chukchi Sea: Distribution Patterns in Seawater and Sediments and Biomagnification in the Benthic Food Web. Deep Sea Research Part II. *Deep Sea Res., Part II* **2014**, *102*, 56−67.
(58) Canário, J.; Poissant, L.; Pilote, M.; Blaise, C.; Constant, P.; Férard, J.-F.; Gagné, F. Toxicity Survey of Canadian Arctic Marine Sediments. *J. Soils Sediments* **2014**, *14* (1), 196−203.
(59) Pirtle-Levy, R.; Grebmeier, J. M.; Cooper, L. W.; Larsen, I. L. Chlorophyll a in Arctic Sediments Implies Long Persistence of Algal Pigments. *Deep Sea Res., Part II* **2009**, *56* (17), 1326−1338.
(60) Polyak, L.; Bischof, J.; Ortiz, J. D.; Darby, D. A.; Channell, J. E. T.; Xuan, C.; Kaufman, D. S.; Løvlie, R.; Schneider, D. A.; Eberl, D. D.; Adler, R. E.; Council, E. A. Late Quaternary Stratigraphy and Sedimentation Patterns in the Western Arctic Ocean. *Global and Planetary Change* **2009**, *68* (1−2), 5−17.
(61) Polyak, L.; Jakobsson, M. Quaternary Sedimentation in the Arctic Ocean: Recent Advances and Further Challenges. *Oceanography* **2011**, *24* (3), 52−64.
(62) Wang, F.; Macdonald, R. W.; Armstrong, D. A.; Stern, G. A. Total and Methylated Mercury in the Beaufort Sea: The Role of Local and Recent Organic Remineralization. *Environ. Sci. Technol.* **2012**, *46* (21), 11821−11828.
(63) Roeske, T.; Rutgers van der Loeff, M.; Middag, R.; Bakker, K. Deep Water Circulation And Composition In The Arctic Ocean By Dissolved Barium, Aluminium And Silicate. *Mar. Chem.* **2012**, *132*−*133*, 56−67.
(64) Schuster, P. F.; Schaefer, K. M.; Aiken, G. R.; Antweiler, R. C.; Dewild, J. F.; Gryziec, J. D.; Gusmeroli, A.; Hugelius, G.; Jafarov, E.; Krabbenhoft, D. P.; Liu, L.; Herman-Mercer, N.; Mu, C.; Roth, D. A.; Schaefer, T.; Striegl, R. G.; Wickland, K. P.; Zhang, T. Permafrost Stores a Globally Significant Amount of Mercury. *Geophys. Res. Lett.* **2018**, *45*, 1463−1471.
(65) Arrigo, K. R.; van Dijken, G. L. Continued Increases in Arctic Ocean Primary Production. *Prog. Oceanogr.* **2015**, *136*, 60−70.
(66) van der Loeff, M. R.; Sarin, M. M.; Baskaran, M.; Benitez-Nelson, C.; Buesseler, K. O.; Charette, M.; Dai, M.; Gustafsson, Ö.; Masque, P.; Morris, P. J.; Orlandini, K.; Rodriguez y Baena, A.; Savoye, N.; Schmidt, S.; Turnewitsch, R.; Vöge, I.; Waples, J. T. A Review of Present Techniques and Methodological Advances in Analyzing ^{234}Th in Aquatic Systems. *Mar. Chem.* **2006**, *100* (3−4), 190−212.
(67) Buesseler, K. O.; Benitez-Nelson, C.; Rutgers van der Loeff, M.; Andrews, J.; Ball, L.; Crossin, G.; Charette, M. A. An Intercomparison of Small- and Large-Volume Techniques for Thorium-234 in Seawater. *Mar. Chem.* **2001**, *74* (1), 15−28.
(68) Pike, S. M.; Buesseler, K. O.; Andrews, J.; Savoye, N. Quantification of ^{234}Th Recovery in Small Volume Sea Water Samples by Inductively Coupled Plasma-Mass Spectrometry. *J. Radioanal. Nucl. Chem.* **2005**, *263* (2), 355−360.

https://dx.doi.org/10.1021/acsearthspacechem.0c00055
ACS Earth Space Chem. XXXX, XXX, XXX−XXX